High Throughput Screening of Semiconductors with Low Lattice Thermal Transport Induced by Long-Range Interactions (Supporting Information)

Yu Wu,*,† Linxuan Ji,‡ Yimin Ding,† and Liujiang Zhou*,‡

†*Yangtze Delta Region Institute (Huzhou), University of Electronic Science and Technology of China, Huzhou 313001, China*

‡*School of Physics and State Key Laboratory of Electronic Thin Films and Integrated Devices, University of Electronic Science and Technology of China, Chengdu 610054, China*

E-mail: wuyu9573@qq.com; ljzhou@uestc.edu.cn

Table S1: The chemical formula, space group, supercell for AIMD calculation, **q**-grid for κ_L calculation, formation energy (FE), average atomic mass and κ_L (300 K) of the screened 75 candidates. The chemical formula labeled with red color represents the material is unstable at 700 K.

Chemical Formula	Space Group	Super Cell	**q**-grid	FE (eV/atom)	Mass (g/mol)	κ_L (W/mK)	ref.
Ag_4O_2	224	$3\times3\times3$	$11\times11\times11$	-0.82	77.25	2.14	
Ag_4O_4	14	$2\times4\times2$	$9\times14\times9$	-1.01	61.93	3.90	
Ag_4O_6	43	$3\times2\times3$	$14\times14\times14$	-1.01	52.75	8.77	
Al_4Ru_2	70	$3\times3\times3$	$13\times13\times13$	-0.83	51.68	14.19	

As_2Mg_3	164	$4 \times 4 \times 2$	$15 \times 15 \times 7$	-0.67	44.55	2.00	
As_4Cd_2	98	$4 \times 4 \times 2$	$13 \times 13 \times 13$	-0.17	87.42	2.53	
As_4Te_6	12	$3 \times 3 \times 2$	$13 \times 13 \times 11$	-0.16	106.53	1.03	
As_8Na_8	19	$2 \times 2 \times 2$	$12 \times 12 \times 9$	-0.99	48.96	0.55	
As_8Na_8	14	$3 \times 2 \times 2$	$12 \times 11 \times 8$	-0.99	48.96	0.84	
As_8Rb_8	19	$2 \times 2 \times 2$	$12 \times 12 \times 9$	-0.52	80.19	0.33	
Ba_2Se_4	15	$4 \times 4 \times 2$	$13 \times 13 \times 13$	-2.03	98.42	1.31	
Bi_1Li_3	225	$3 \times 4 \times 3$	$13 \times 13 \times 13$	-1.24	57.50	1.67	2.1[1]
Bi_2Se_3	166	$3 \times 3 \times 3$	$14 \times 14 \times 14$	-1.16	130.97	2.32	1.33[2]
Bi_4I_4	12	$3 \times 3 \times 2$	$13 \times 13 \times 6$	-1.06	167.94	0.82	
Bi_4Se_8	12	$2 \times 2 \times 3$	$13 \times 13 \times 6$	-1.04	122.30	0.34	
Br_4Te_2	136	$3 \times 2 \times 5$	$9 \times 9 \times 16$	-0.68	95.80	1.25	
C_4Os_4	198	$3 \times 3 \times 2$	$11 \times 11 \times 11$	-0.73	101.11	22.16	
Ca_2Ge_1	225	$4 \times 4 \times 4$	$12 \times 12 \times 12$	-1.02	50.92	5.73	
Ca_2Si_1	225	$4 \times 4 \times 4$	$12 \times 12 \times 12$	-0.89	36.08	8.66	
Cl_2Cu_1	12	$5 \times 5 \times 2$	$17 \times 17 \times 8$	-1.15	44.82	6.21	
Co_6O_8	227	$2 \times 2 \times 3$	$11 \times 11 \times 11$	-2.64	34.40	1.32	
Cr_3Si_6	180	$3 \times 3 \times 2$	$15 \times 15 \times 8$	-1.44	36.06	20.51	
Cr_3Si_6	181	$3 \times 3 \times 2$	$15 \times 15 \times 8$	-1.44	36.06	21.22	
Cs_4Te_{16}	14	$2 \times 3 \times 2$	$11 \times 12 \times 9$	-0.55	128.66	0.28	
Cu_4O_2	224	$3 \times 3 \times 3$	$12 \times 12 \times 12$	-2.25	47.70	4.43	
F_4Hg_2	136	$3 \times 3 \times 3$	$10 \times 10 \times 13$	-1.93	79.53	1.90	
F_6Mn_2	55	$2 \times 3 \times 3$	$9 \times 9 \times 13$	-3.92	27.98	7.64	
Fe_4Si_4	198	$2 \times 3 \times 3$	$11 \times 11 \times 11$	-1.11	41.97	22.62	
Ga_4Os_2	70	$3 \times 3 \times 3$	$14 \times 14 \times 14$	-0.38	109.88	8.40	
Ge_1Mg_2	225	$4 \times 4 \times 4$	$14 \times 14 \times 14$	-0.45	40.41	8.49	5.6[3]
Ge_1Se_1	160	$5 \times 5 \times 5$	$16 \times 16 \times 16$	-0.51	75.79	6.30	4.53[4]

Ge_1Te_1	160	$5 \times 5 \times 5$	$16 \times 16 \times 16$	-0.41	100.10	5.56	
Ge_4O_8	205	$2 \times 2 \times 3$	$11 \times 11 \times 11$	-2.78	34.87	14.35	
Ge_4Se_4	62	$2 \times 4 \times 3$	$5 \times 21 \times 21$	-0.75	75.78	2.48	
Hf_1Se_2	164	$5 \times 5 \times 2$	$27 \times 27 \times 7$	-1.80	112.14	5.63	
Hf_2Se_6	11	$3 \times 4 \times 2$	$11 \times 15 \times 7$	-1.50	103.84	4.55	
In_4S_4	64	$3 \times 3 \times 2$	$13 \times 13 \times 6$	-1.15	73.44	1.99	
I_4Te_2	136	$2 \times 3 \times 5$	$9 \times 9 \times 15$	-0.40	127.14	2.57	
Ir_4N_8	14	$2 \times 3 \times 2$	$11 \times 10 \times 11$	-3.17	73.41	25.43	
K_4O_2	141	$3 \times 3 \times 3$	$10 \times 10 \times 14$	-1.84	31.40	2.19	
K_6Te_6	189	$2 \times 2 \times 3$	$11 \times 11 \times 10$	-1.11	83.35	0.38	
K_8Te_{12}	62	$1 \times 2 \times 4$	$8 \times 10 \times 16$	-0.97	92.20	0.34	
Li_3Sb_1	225	$4 \times 3 \times 3$	$15 \times 15 \times 15$	-1.36	35.70	2.04	2.2[1]
Li_8P_8	14	$2 \times 2 \times 2$	$12 \times 12 \times 8$	-2.58	18.99	2.02	
Mg_1Te_1	225	$4 \times 4 \times 4$	$15 \times 15 \times 15$	-0.91	75.95	2.88	
Mg_2Si_1	225	$4 \times 4 \times 4$	$14 \times 14 \times 14$	-0.36	25.56	11.31	
Mg_3Sb_2	164	$4 \times 4 \times 2$	$16 \times 16 \times 15$	-0.84	63.28	1.93	
Mo_3Si_6	180	$3 \times 3 \times 2$	$15 \times 15 \times 8$	-1.08	50.70	14.96	
N_4Pt_2	58	$3 \times 2 \times 4$	$13 \times 10 \times 16$	-3.06	74.36	142.29	
N_6W_3	152	$3 \times 3 \times 2$	$12 \times 12 \times 8$	-3.80	70.62	5.07	
N_8W_4	33	$2 \times 3 \times 2$	$11 \times 9 \times 11$	-3.82	70.62	7.35	
Na_6S_6	189	$2 \times 2 \times 3$	$11 \times 11 \times 11$	-2.02	27.53	1.67	
Na_8P_8	19	$3 \times 2 \times 2$	$12 \times 11 \times 8$	-2.68	26.98	0.89	
$O_{11}Zr_6$	25	$3 \times 3 \times 1$	$16 \times 16 \times 5$	-4.50	42.55	3.04	
O_2Pd_2	131	$5 \times 5 \times 2$	$16 \times 16 \times 9$	-1.56	61.21	84.21	
O_2Pt_2	131	$4 \times 4 \times 2$	$16 \times 16 \times 9$	-1.38	105.54	66.01	
O_6Pb_4	31	$5 \times 2 \times 2$	$15 \times 8 \times 10$	-2.06	92.48	0.89	
O_6Ti_4	167	$2 \times 3 \times 3$	$11 \times 11 \times 11$	-4.08	28.75	7.64	

$O_{12}Ti_8$	62	$2 \times 2 \times 2$	$8 \times 19 \times 8$	-4.03	28.75	5.17	
Os_2P_4	58	$2 \times 3 \times 5$	$10 \times 8 \times 17$	-2.98	84.05	30.53	
Os_4Si_4	198	$3 \times 3 \times 2$	$11 \times 11 \times 11$	-0.80	109.14	16.76	
Pb_1Se_1	225	$4 \times 4 \times 4$	$14 \times 14 \times 14$	-0.93	143.08	2.88	1.7[5]
Pb_1Te_1	225	$4 \times 4 \times 4$	$13 \times 13 \times 13$	-0.55	167.40	3.84	2.6[5]
Pb_2S_2	186	$5 \times 5 \times 2$	$15 \times 15 \times 7$	-1.20	119.63	1.76	
Rb_2Te_5	12	$3 \times 2 \times 3$	$10 \times 10 \times 13$	-0.68	115.56	0.48	
Rb_6Te_6	189	$2 \times 2 \times 3$	$11 \times 11 \times 10$	-0.96	106.53	0.39	
Ru_4Si_4	198	$2 \times 3 \times 3$	$11 \times 11 \times 11$	-1.05	64.58	12.88	
Sc_4Se_6	15	$3 \times 3 \times 2$	$11 \times 11 \times 10$	-2.14	65.36	1.76	
Sc_4Te_6	15	$2 \times 3 \times 3$	$11 \times 11 \times 10$	-1.40	94.54	1.09	
Se_2Sn_2	63	$4 \times 3 \times 3$	$12 \times 12 \times 12$	-0.77	98.83	1.27	0.9[6]
Se_2Sn_2	129	$5 \times 5 \times 2$	$18 \times 18 \times 7$	-0.73	98.83	2.98	
Se_2Zr_1	164	$5 \times 5 \times 2$	$18 \times 18 \times 7$	-1.78	83.05	5.57	
Se_4Sn_4	62	$2 \times 4 \times 3$	$6 \times 14 \times 13$	-0.78	98.83	2.42	1.3[6]
Se_6Zr_2	11	$3 \times 4 \times 2$	$11 \times 15 \times 7$	-1.53	82.03	4.48	
Si_6W_3	180	$3 \times 3 \times 2$	$15 \times 15 \times 8$	-0.77	80.01	11.83	

Table S2: The chemical formula, space group, supercell for AIMD calculation, **q**-grid for κ_L calculation, formation energy (FE), average atomic mass and κ_L (300 K) of the screened 26 candidates without LRI.

Chemical Formula	Space Group	Super Cell	**q**-grid	FE (eV/atom)	Mass (g/mol)	κ_L (W/mK)
Al_2Os_1	139	$3 \times 3 \times 5$	$14 \times 14 \times 19$	-0.74	81.39	10.53
As_1Ga_1	216	$4 \times 4 \times 4$	$15 \times 15 \times 15$	-0.44	72.32	40.92
As_2K_6	194	$3 \times 3 \times 2$	$14 \times 14 \times 7$	-0.62	48.05	0.61
As_2Li_6	194	$3 \times 3 \times 2$	$15 \times 15 \times 6$	-1.18	23.99	3.92

B_1Sb_1	216	$4 \times 4 \times 4$	$15 \times 15 \times 15$	-0.34	66.28	457.17
C_1Hf_1	216	$4 \times 4 \times 4$	$15 \times 15 \times 15$	-1.78	95.25	77.13
C_1Ru_1	216	$4 \times 4 \times 4$	$15 \times 15 \times 15$	-1.09	56.54	41.68
C_1Zr_1	216	$4 \times 4 \times 4$	$15 \times 15 \times 15$	-1.67	51.62	98.17
Fe_2Sb_4	58	$2 \times 2 \times 5$	$10 \times 9 \times 17$	-1.48	99.78	9.12
Fe_2Te_4	58	$3 \times 2 \times 4$	$10 \times 9 \times 14$	-0.65	103.68	11.51
Ga_1Sb_1	216	$4 \times 4 \times 4$	$14 \times 14 \times 14$	-0.74	95.74	49.19
Ga_4Se_4	187	$5 \times 5 \times 1$	$19 \times 19 \times 4$	-0.92	74.34	16.71
Ge_2Si_2	186	$5 \times 5 \times 2$	$18 \times 18 \times 8$	-0.46	50.35	106.45
In_1P_1	216	$4 \times 4 \times 4$	$15 \times 15 \times 15$	-2.00	72.90	90.86
In_2P_2	186	$5 \times 5 \times 2$	$15 \times 15 \times 7$	-1.99	72.90	80.78
In_4Se_4	194	$5 \times 5 \times 1$	$17 \times 17 \times 5$	-0.83	96.89	11.83
K_3Sb_1	225	$3 \times 3 \times 3$	$11 \times 11 \times 11$	-0.94	59.76	0.93
K_4Te_4	194	$3 \times 3 \times 2$	$15 \times 15 \times 7$	-1.10	83.35	0.48
K_6Sb_2	194	$3 \times 3 \times 2$	$14 \times 14 \times 7$	-0.96	59.76	0.51
Li_6P_2	194	$3 \times 3 \times 2$	$15 \times 15 \times 7$	-2.01	13.00	4.03
Mo_2Te_4	194	$5 \times 5 \times 1$	$19 \times 19 \times 4$	-0.64	117.05	15.72
Ni_2P_4	15	$2 \times 3 \times 3$	$13 \times 13 \times 16$	-2.82	40.21	26.32
P_4Pd_2	15	$3 \times 3 \times 2$	$13 \times 13 \times 10$	-2.81	56.12	23.22
Pt_2S_2	131	$5 \times 5 \times 2$	$14 \times 14 \times 8$	-1.18	113.57	58.20
Ru_2Te_4	58	$3 \times 2 \times 4$	$11 \times 10 \times 14$	-0.58	118.76	18.34
Si_1Sn_1	216	$4 \times 4 \times 4$	$14 \times 14 \times 14$	-0.17	73.40	83.18

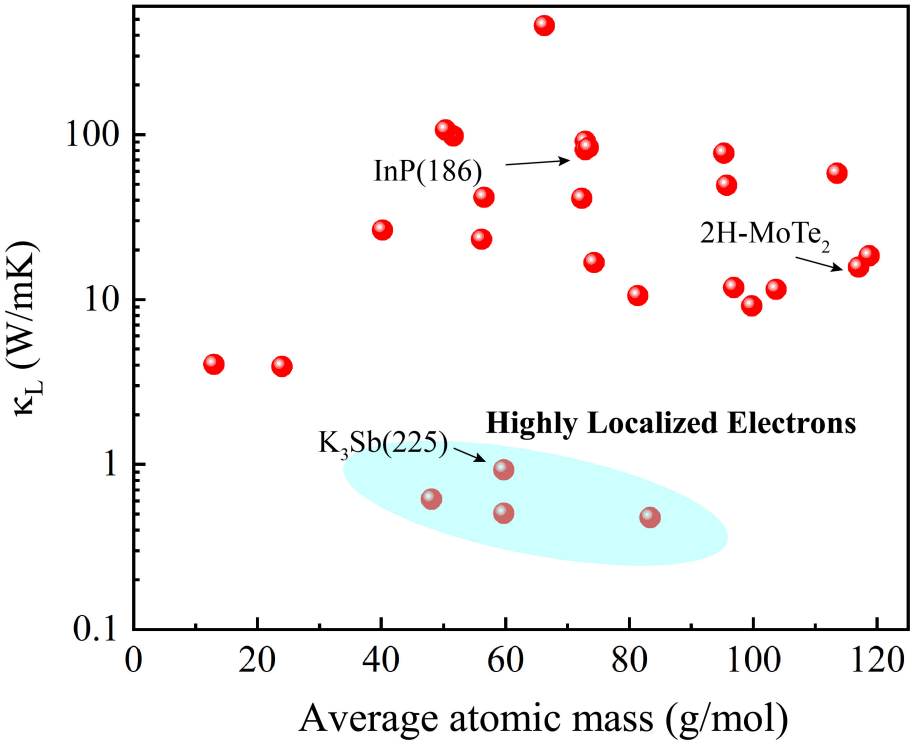

Figure S1: The κ_L of 26 materials without LRI versus the average atomic mass at 300K. The blue areas represent highly localized electrons in the material with extremely flat valence bands.

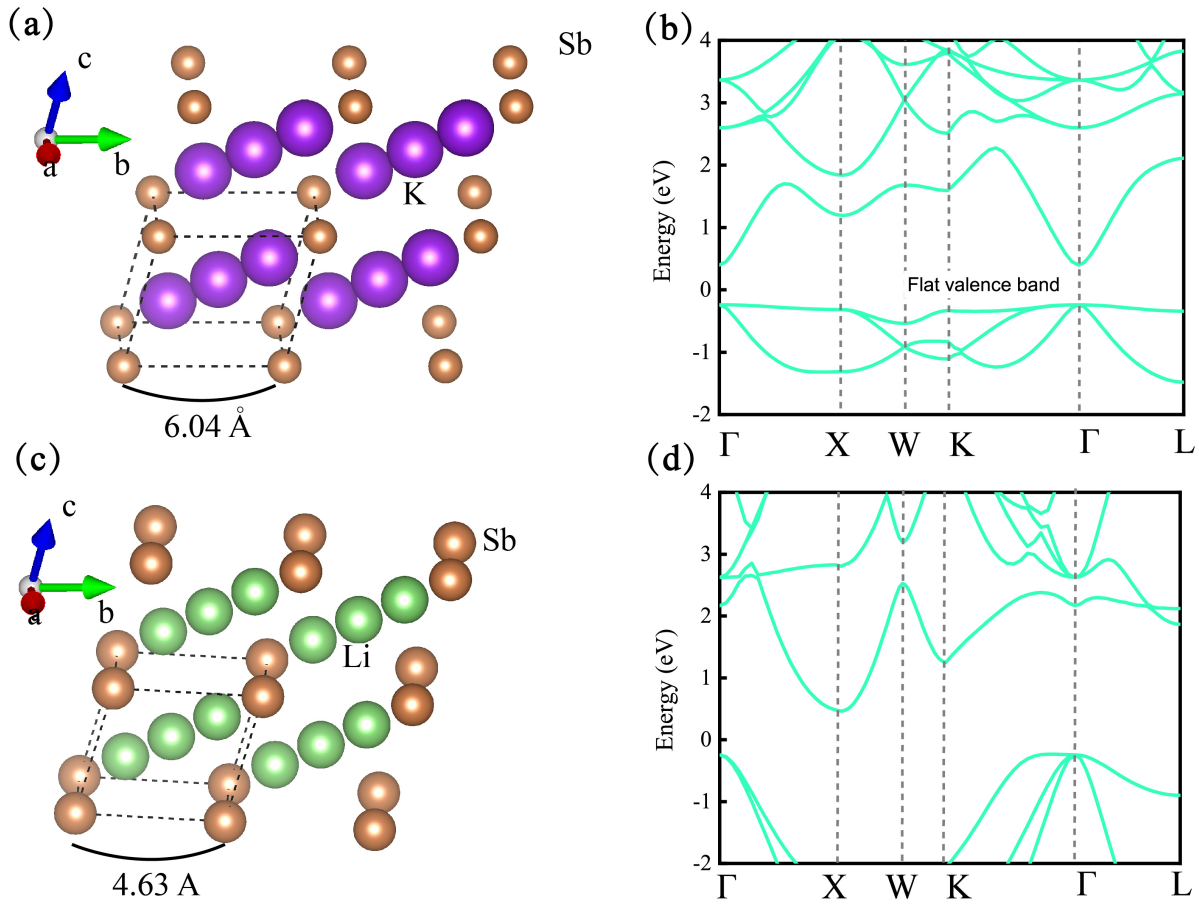

Figure S2: (a) Crystal structure and (b) band structure of K_3Sb. (c) Crystal structure and (d) band structure of Li_3Sb.

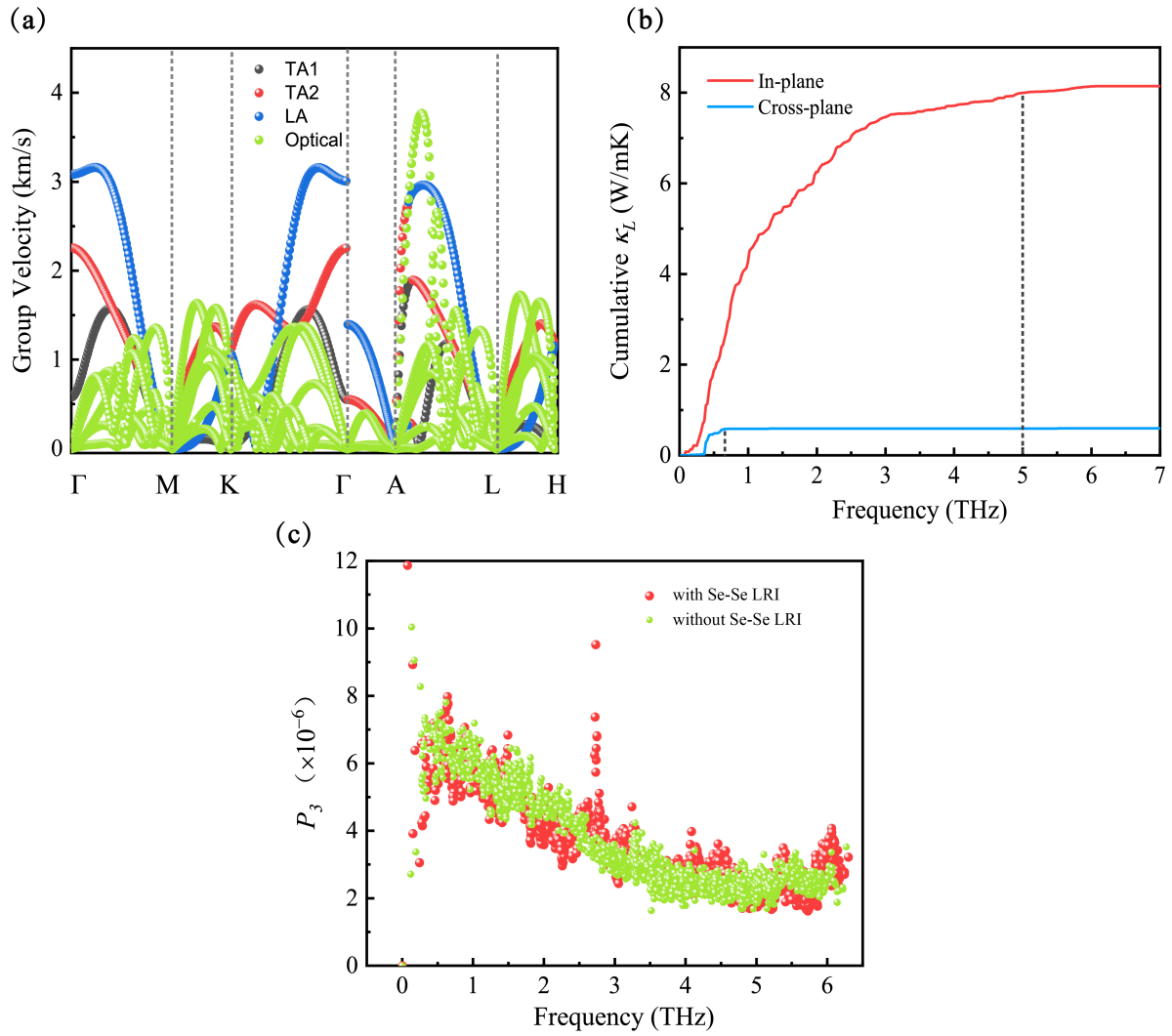

Figure S3: (a) The mode-resolved group velocity of $HfSe_2$ along the high symmetry path. (b) Frequency dependence of cumulative κ_L. (c) Phase space of $HfSe_2$ with and without the LRI of Se-Se.

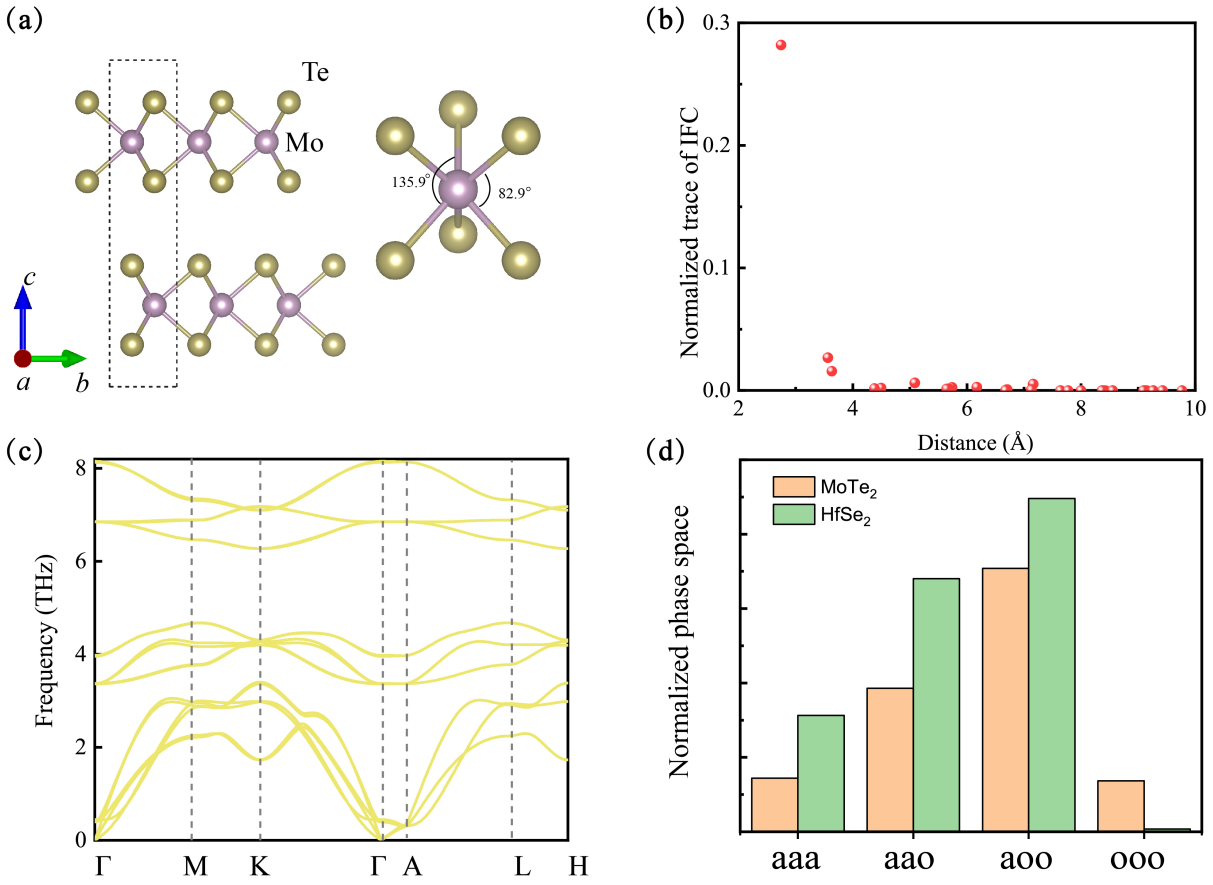

Figure S4: (a) Crystal structure of 2H-$MoTe_2$. (b) Normalized trace of IFCs versus atomic distance at 300 K for the Te atom. (c) Phonon dispersion for 2H-$MoTe_2$ at 300 K. (d) Normalized channel resolved phase space for 2H-$MoTe_2$ and $HfSe_2$.

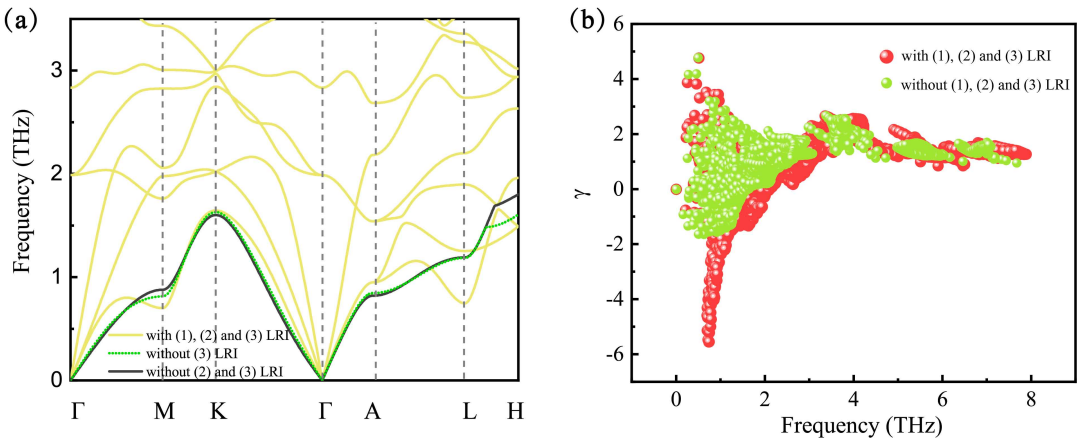

Figure S5: (a) Phonon dispersion of Mg_3Sb_2 with (1), (2), (3) LRI, without (3) and without (2), (3) LRI. The used cut-off radii are 10.00 Å, 5.90 Å and 4.79 Å, respectively. (b) The frequency dependent Grüneisen parameters with and without (1), (2), (3) LRI. The cut-off radii are used 10.00Å and 4.59 Å, respectively.

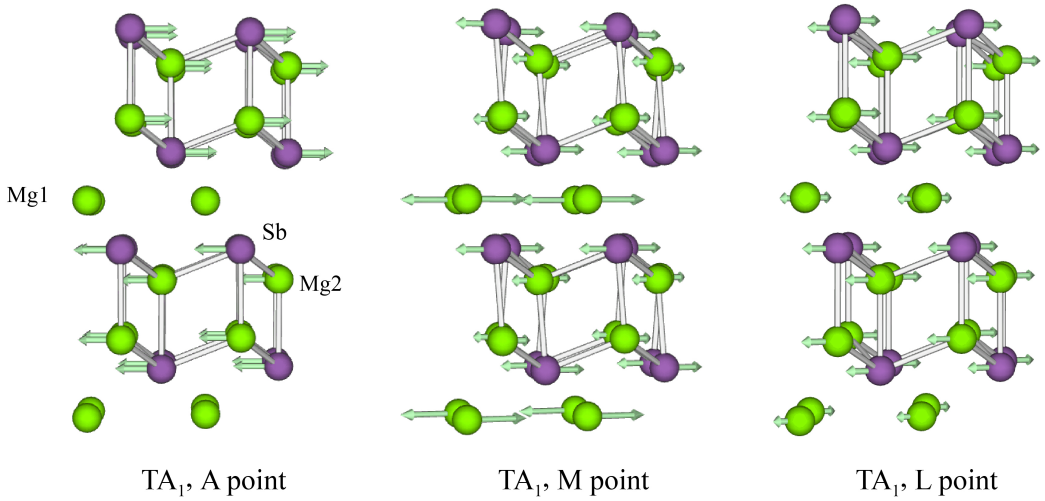

Figure S6: Visualization of vibration modes for Mg_3Sb_2.

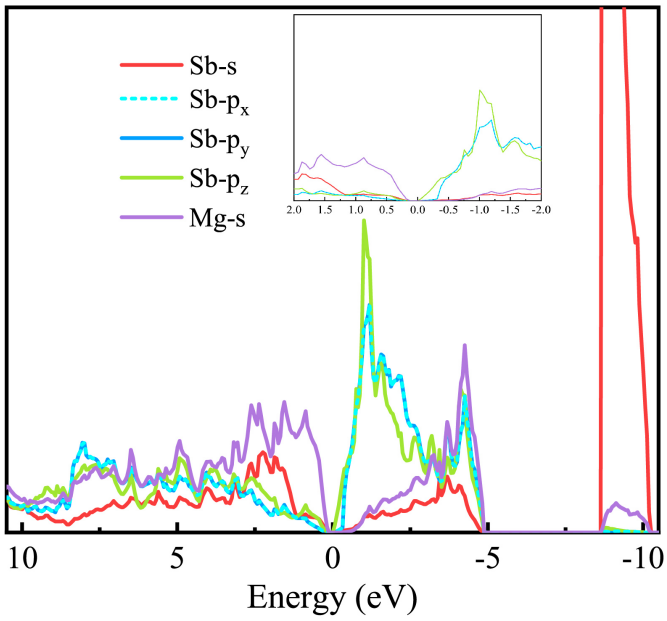

Figure S7: Electronic DOS of Mg_3Sb_2 contributed by Mg-s, Sb-s and Sb-p orbitals.

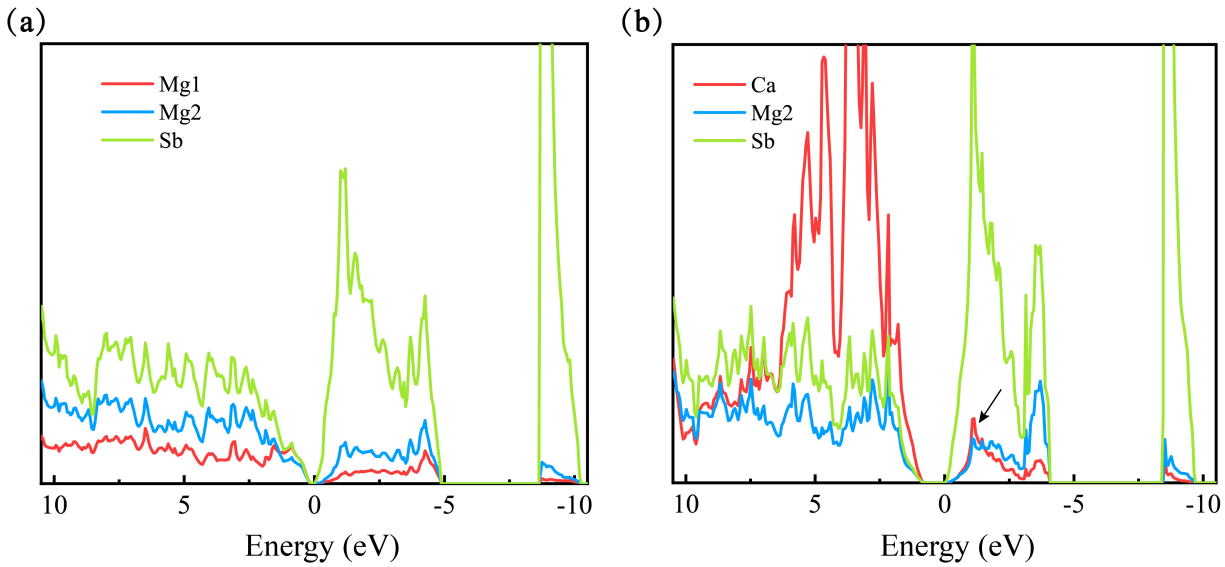

Figure S8: Electronic DOS of Mg_3Sb_2 and $CaMg_2Sb_2$ contributed by A, M and X-site atoms in formula AM_2X_2.

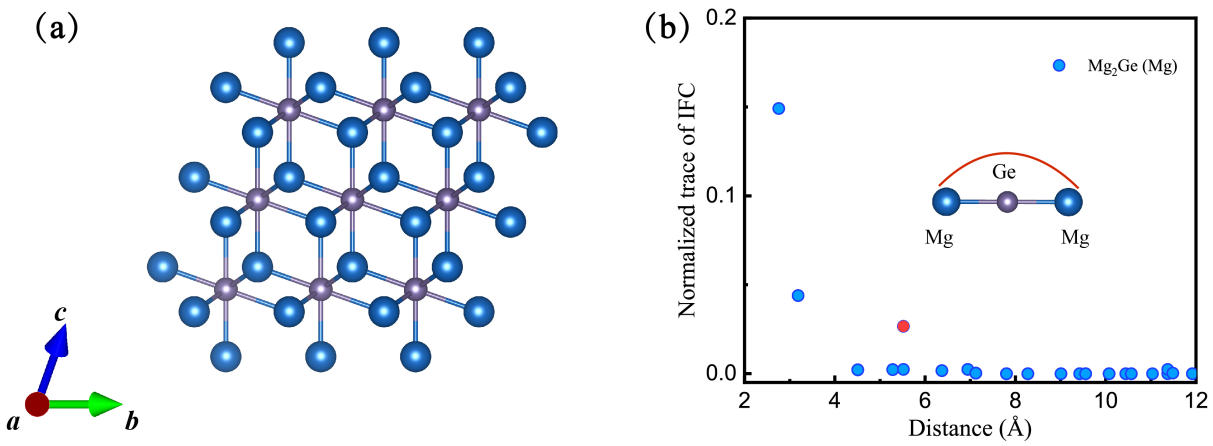

Figure S9: (a) Crystal structure of Mg_2Ge from side view. (b) Normalized trace of IFCs versus atomic distance for Mg atom.

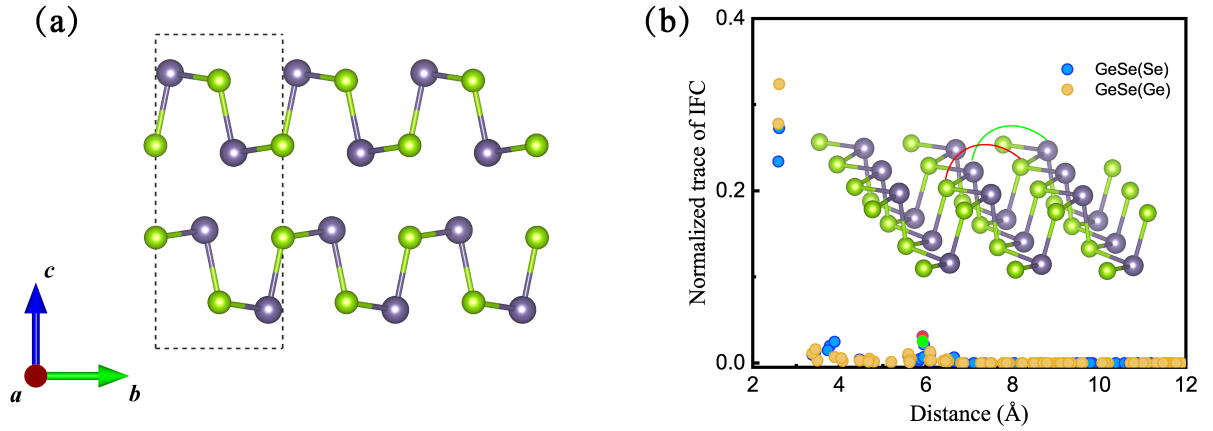

Figure S10: (a) Crystal structure of *Pnma*-GeSe from side view. (b) Normalized trace of IFCs versus atomic distance for Se and Ge atoms.

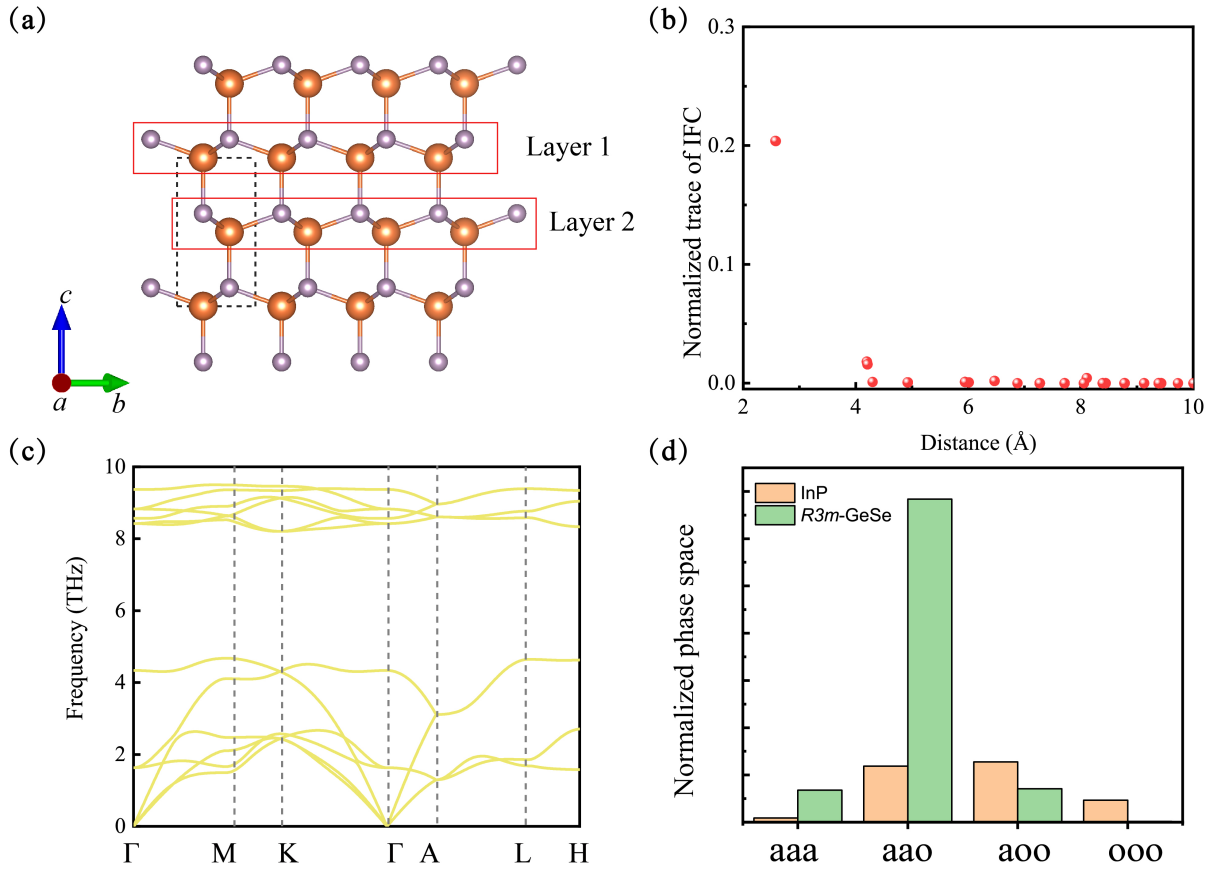

Figure S11: (a) Crystal structure of InP with space group 186. (b) Normalized trace of IFCs versus atomic distance at 300 K for the P atom. (c) Phonon dispersion for InP at 300 K. (d) Normalized channel resolved phase space for InP and $R3m$-GeSe.

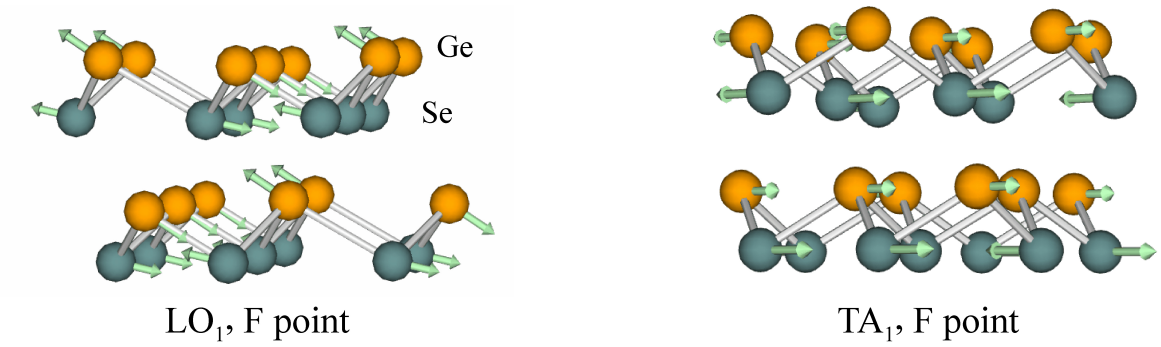

Figure S12: Visualization of vibration modes for $R3m$-GeSe.

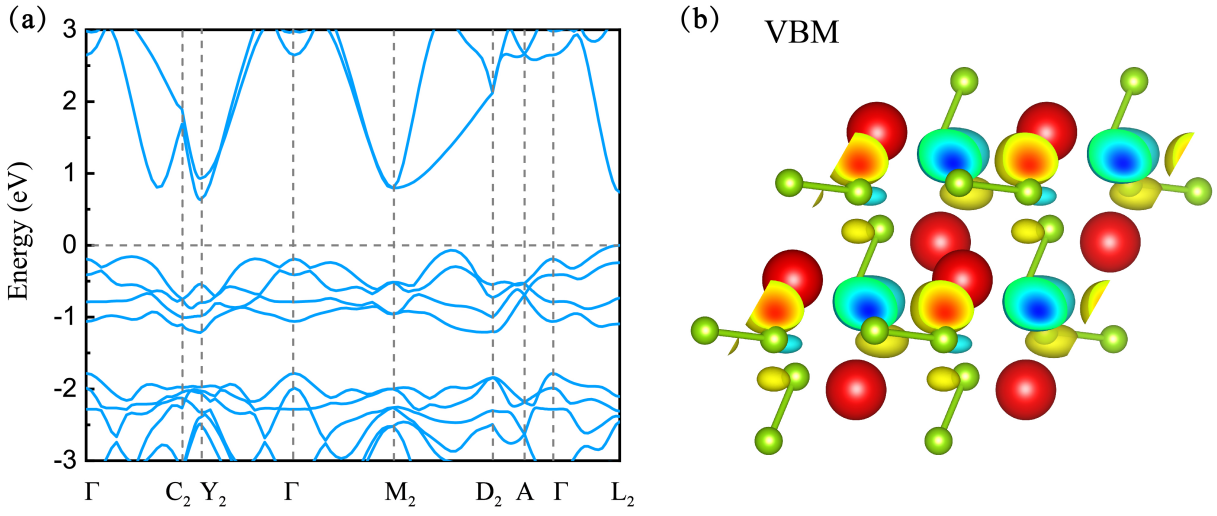

Figure S13: (a) The band structure of $BaSe_2$. (b) The isosurfaces of the VBM electronic wavefunctions.

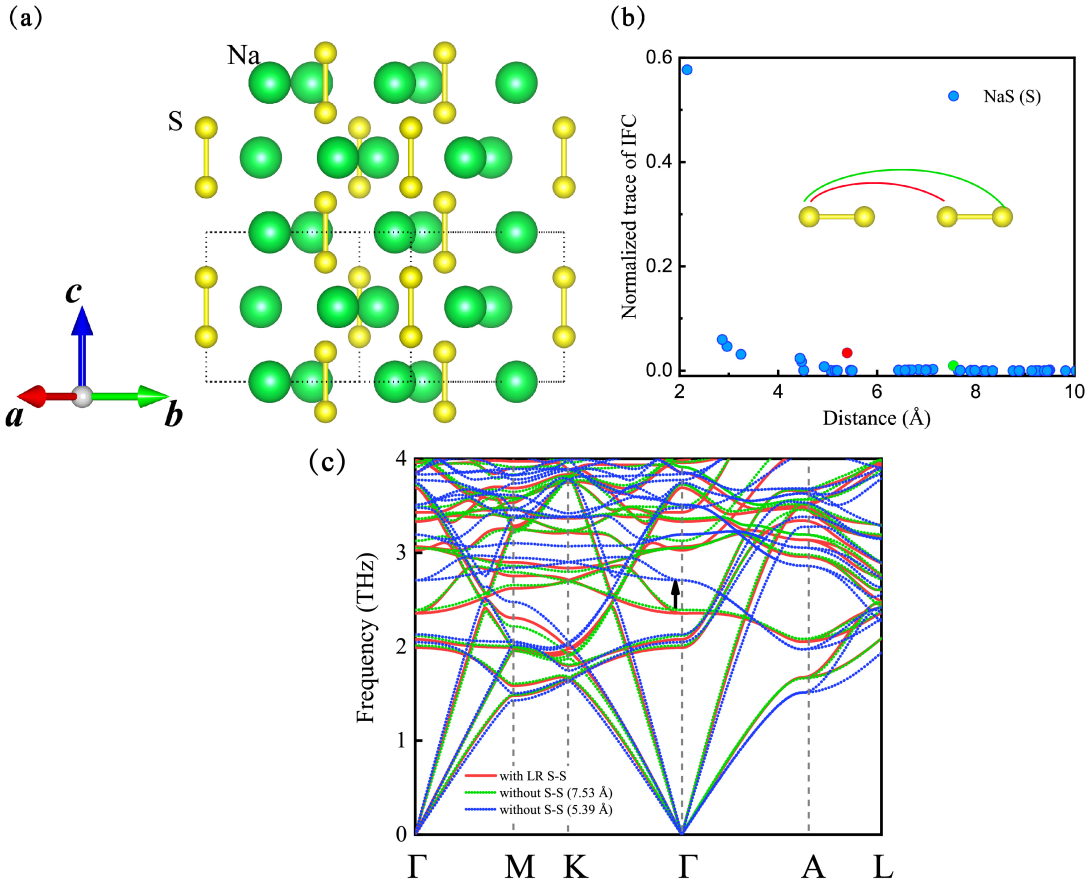

Figure S14: (a) Crystal structure of NaS from side view. (b) Normalized trace of IFCs versus atomic distance for S atoms. (c) Phonon dispersion of NaS with S-S LRI, without Se-Se (7.53 Å), and without Se-Se (5.39 Å) LRI at 300 K. The used cut-off radii are 10.00 Å, 7.52 Å and 5.38 Å, respectively.

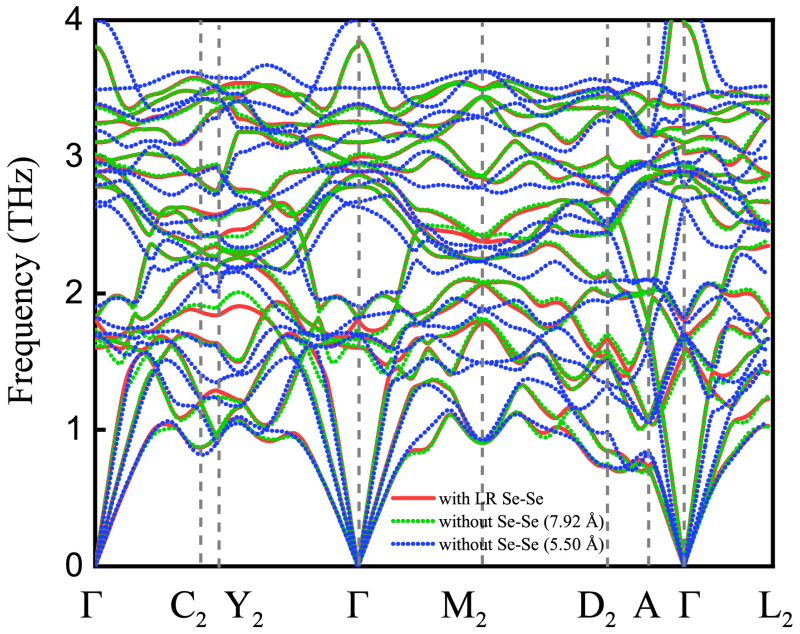

Figure S15: Phonon dispersion of $BaSe_2$ with Se-Se LRI, without Se-Se (7.92Å) and without Se-Se (5.50 Å) LRI at 300 K. The used cut-off radii are 10.00Å, 7.91Å and 5.49 Å, respectively.

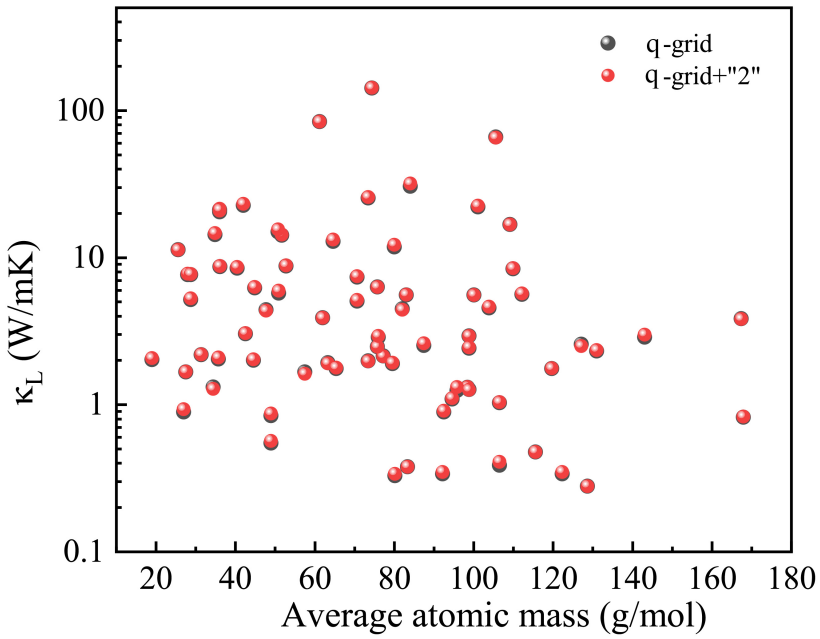

Figure S16: The calculated κ_L of the screened 75 materials with the **q**-grid in Table S1 and the **q**-grid in Table S1 to add 2 in each of the three directions.

References

(1) Yang, X.; Dai, Z.; Zhao, Y.; Liu, J.; Meng, S. Low lattice thermal conductivity and excellent thermoelectric behavior in Li3Sb and Li3Bi. *J. Phys. Condens. Matter* **2018**, *30*, 425401.

(2) Navrátil, J.; Horák, J.; Plecháček, T.; Kamba, S.; Lošt'ák, P.; Dyck, J.; Chen, W.; Uher, C. Conduction band splitting and transport properties of Bi2Se3. *J. Solid State Chem.* **2004**, *177*, 1704–1712.

(3) Rittiruam, M.; Vora-Ud, A.; Impho, W.; Seetawan, T. Prediction of thermal conductivity of Mg2X (X = Ge and Sn) by molecular dynamics. *Integr. Ferroelectr.* **2015**, *165*, 61–72.

(4) Zhang, M.; Flitcroft, J. M.; Guillemot, S. K.; Skelton, J. M. Thermoelectric properties of Pnma and R3m GeS and GeSe. *J. Mater. Chem. C* **2023**, *11*, 14833–14847.

(5) Shulumba, N.; Hellman, O.; Minnich, A. J. Intrinsic localized mode and low thermal conductivity of PbSe. *Phys. Rev. B* **2017**, *95*, 014302.

(6) Skelton, J. M.; Burton, L. A.; Parker, S. C.; Walsh, A.; Kim, C.-E.; Soon, A.; Buckeridge, J.; Sokol, A. A.; Catlow, C. R. A.; Togo, A.; Tanaka, I. Anharmonicity in the high-temperature *Cmcm* phase of SnSe: Soft modes and three-phonon interactions. *Phys. Rev. Lett.* **2016**, *117*, 075502.